

## **Parameterization of Spatio-temporal Patterns of Volcanic Aerosol Induced Stratospheric Optical Depth and its Climate Radiative Forcing**

**JÜRGEN GRIESER AND CHRISTIAN-D. SCHÖNWIESE**

*Department of Meteorology and Geophysics, University of Frankfurt,  
P.O. Box 11 19 32, 60054 Frankfurt, Germany*

(Manuscript received May 12, 1998; accepted in final form Sept. 21, 1998)

### **RESUMEN**

Se sabe que el vulcanismo explosivo tiene un gran impacto sobre el clima. Así, para entender la variabilidad climática del pasado, el forzamiento volcánico tiene que tomarse en cuenta. Se dispone de los datos instrumentales del espesor óptico de los aerosoles estratosféricos para las más recientes erupciones volcánicas explosivas. Para erupciones antiguas existen sólo indicativos con ninguna o solamente una burda resolución espacial y temporal. Para estimar los patrones espacio-temporales del espesor óptico inducido por los aerosoles de la atmósfera debidos a alguna erupción volcánica fuerte conocida, introducimos una parametrización de la distribución de los aerosoles estratosféricos, mediante el uso de información reciente acerca de los fenómenos de transporte estratosféricos, así como la fecha, ubicación y fuerza de una erupción.

Empleando esta parametrización se pueden reproducir con exactitud razonable series de tiempo observadas del espesor óptico de los aerosoles estratosféricos. Para investigar el forzamiento volcánico del clima, introducimos una parametrización de la transferencia irradiativa que toma en cuenta el patrón estacional y latitudinal, no perturbado, de la absorción de la radiación, así como la extensión de la trayectoria de un rayo en una capa esférica. Así pues, los patrones espacio-temporales del forzamiento volcánico del clima pueden estimarse, también para cualquier erupción volcánica conocida.

### **ABSTRACT**

Explosive volcanism is known to have a large impact on climate. Thus, in order to understand past climate variability, volcanic forcing has to be considered. For the most recent explosive volcanic eruptions instrumental data of stratospheric aerosol optical depth are available. For early eruptions only index values with no or only crude spatial and seasonal resolution do exist. To estimate the spatio-temporal patterns of aerosol induced optical depth of the atmosphere due to any known strong volcanic eruption, we introduce a stratospheric aerosol distribution parameterization using recent information about stratospheric transport phenomena as well as date, location, and strength of an eruption. Using this parameterization, observed time series of stratospheric aerosol optical depth can be reproduced with reasonable accuracy.

To investigate volcanic climate forcing, we introduce a radiation transfer parameterization which takes into account the undisturbed seasonal and latitudinal pattern of radiation uptake as well as the extension of a ray path in a spherical layer. Thus, spatio-temporal patterns of volcanic climate forcing for any known volcanic eruption can be estimated, too.

## 1. Introduction

Knowledge about strong explosive volcanic eruptions is important in many scientific fields because these eruptions may be dangerous for human life and property and therefore may also be of socio-economic consequences. Apart from the direct effects in the surrounding of an erupting volcano there is also a climatic impact caused by stratospheric aerosol clouds which can be produced by strong eruptions. The strongest volcanic eruption of the past 200 years was the Tambora eruption in April 1815. The following year is known as the "year without summer" (Stommel and Stommel, 1979). However, less powerful eruptions have an impact on the climate, too. Thus, long time series of both, volcanic activity induced perturbations of the atmosphere and related climate forcing, are needed to understand volcano-climate relationships.

Moreover, in order to interpret anthropogenic climate change, it is necessary to understand natural influences like volcanism which are in competition with anthropogenic forcing. Explosive volcanism is known to have a strong influence on the temperature of the atmosphere. This problem is discussed in many papers (e.g. Hansen and Lacis, 1990; Sato *et al.*, 1993; Jones and Kelly, 1996). In spite of that, explosive volcanic forcing is usually considered in terms of index value time series as a tool for the evaluation and analysis of climate parameter time series (Jones and Kelly, 1996; Tol and de Vos, 1998).

These index value time series are the dust veil index (*DVI*) proposed by Lamb (1970, 1977, 1983), the severity index by Mitchell (1970), the volcanic explosivity index (*VEI*) by Simkin *et al.* (1981) or Newhall and Self (1982), the smithsonian volcanic index (*SVI*) by Schönwiese (1988), or Cress and Schönwiese (1992) and the ice core volcanic index (*IVI*) by Robock and Free (1995). The latter paper also involves a comprehensive overview of the differences between these various index time series. Most of the information provided by these index time series does not address atmospheric radiation transmission processes and therefore these time series have to be seen as only a crude approximation of volcanic forcing of the climate system. Nevertheless, in very recent investigations these index values are used to offer a statistical explanation of global temperature variations caused by explosive volcanic eruptions (e.g. Tol and De Vos, 1998).

This kind of approach may be appropriate for a statistical analysis and of interest in the case of unknown physical relations between volcanic forcing and related climate parameters. But if one is interested in a more quantitative analysis of past climate variations one has to know the spatio-temporal patterns of volcanic forcing in more detail. Because the volcanic aerosol changes the radiation budget of the atmosphere, it is important to know at least its aerosol optical depth (*AOD*) as a bulk property (Rind, 1996). Since 1961 measurements of atmospheric radiation extinction are available from sites in both hemispheres (Dyer and Hicks, 1968). The NIMBUS 7 satellite provides data from polar regions since 1979 (Stratospheric Aerosol Monitor, SAM II; McCormick *et al.*, 1979, and McCormick, 1994). The Stratospheric Aerosol and Gas Experiment (SAGE II, McCormick and Wang, 1987) provides data between about  $70^{\circ}N$  and  $70^{\circ}S$  since 1984. If one is interested in volcanic *AOD* before 1961 one has to reconstruct this property from other information sources. This is done for example by Sato *et al.* (1993) and Stothers (1996). Sato *et al.* (1993) provide annual mean stratospheric *AOD* with respect to the wavelength  $\lambda = .55\mu m$  for four equal-area zones from 1850 to 1990 and take into account different kinds of information. They also give an actualized version on a 24-point latitude grid with monthly resolution from 1850 to 1999 (Sato, 1995). The last five years of the record contain only an exponential decay of the last observations in 1994. Nevertheless, for the period from 1850 to 1882 they only use the rescaled index from Mitchell (1970) which has no spatial resolution. Therefore Sato *et al.* (1993) provide global averaged values for the time before 1890. Stothers (1996) evaluates volcanic stratospheric *AOD* from 1881 to 1933 from pyrhelimetric data at several stations. Together with the more recent index values evaluated by Sato (1995), this seems to be the most reliable spatial *AOD* time series available today. Nevertheless, both Sato (1995) and Stothers (1996) find different spatio-temporal *AOD* patterns, as will be shown in section 4.

The disadvantage of low (or no) spatial resolution of *AOD* patterns due to volcanic eruptions before the availability of instrumental data can be avoided by using the information of the strength, date, and location of volcanic eruptions as well as by introducing a stratospheric transport parameterization. Date and location of volcanic eruptions are available with fair accuracy from the Volcanic Explosivity Index (*VEI*, Simkin *et al.*, 1981). However, the explosivity given by *VEI* is not a reliable measure of the stratospheric aerosol loading for two reasons. First, stratospheric mass loading is assumed to be proportional to  $10^{VEI}$  (and *VEI* is given in integers. Thus an error in *VEI* leads to an error of at least a factor 10 in respect to the estimated stratospheric volcanic mass loading). Second, *VEI* says nothing about the amount of precursors to build stratospheric aerosol (Robock and Free, 1995). Nevertheless, for recent eruptions *VEI* can be corrected with the help of other information available (see section 2). For the spatial and temporal evolution of the stratospheric aerosol cloud the season and latitude of the eruption seem to be most important (Bradley, 1988).

Thus, we obtain a more detailed spatial resolution of *AOD* of historical eruptions by using a stratospheric transport parameterization (which is introduced in section 2) and information about location, date and strength of volcanic eruptions, although the latter information is not very reliable. Furthermore, the stratospheric transport parameterization can be used for further investigations of any past volcanic eruptions known. The parameterization is calibrated with respect to different information available about stratospheric transport mechanisms and the most recent eruptions of El Chichón (1982) and Mount Pinatubo (1991).

In principle, the time series of spatial patterns of *AOD* can be used to drive a general circulation model (GCM). So far, transient calculations are carried out by Hansen *et al.* (1996) with a pure atmospheric GCM. In addition, coupled atmospheric-oceanic GCM simulations under January and July conditions, respectively, do exist (Graf *et al.*, 1996). But due to its large numerical effort and computation time such GCM runs can only be case studies. Therefore, no long-term GCM calculations of the volcanic impact on climate do exist. That is why simplified models have to be used. Stenchikov *et al.* (1997) found from GCM calculations that the aerosol radiative forcing following the Pinatubo eruption (1991) is not sensitive to the dynamical atmospheric response to this forcing. This encourages radiative forcing calculations without using GCMs.

To obtain an estimate of volcanic forcing one can use the crude approximation of Lacis *et al.* (1992) to get the net radiative flux change at the tropopause  $\Delta F_{net}$  for the case of a uniform aerosol layer:

$$\Delta F_{net}(W/m^2) \approx 30 \cdot \tau_{.55} \quad (1)$$

where  $\tau_{.55}$  is the *AOD* at the wavelength  $\lambda = .55\mu m$ . This approximation neglects the seasonal and latitudinal dependence of the undisturbed radiation uptake. In order to obtain a time series of volcanic forcing not as crude as when using the approximation (1) but with much less numerical effort and computer time as it is needed in a GCM or a radiative-convective model, a simple solution of the radiation-transfer equation (RTE) is introduced (see section 3).

Finally, using the RTE solution with respect to the *AOD* time series, we obtain estimates of spatio-temporal patterns of volcanic forcing in  $W/m^2$  (section 4).

## 2. Volcanic aerosol optical depth

### 2.1 Assessments of volcanic aerosol mass loading of the stratosphere

In order to estimate time series of the spatial patterns of volcanic aerosol optical depth (*AOD*)

variations of the stratosphere we assume that  $AOD$  is linearly proportional to the volcanic aerosol mass concentration  $a$ ,

$$AOD = p_1 \cdot a, \quad (2)$$

where  $p_1$  is a scale factor. To calculate horizontal space-time patterns of the volcanic aerosol mass concentration following an eruption, we use a stratospheric transport parameterization to describe the spreading of the aerosol within the lower to mid-stratosphere, presented in section 2.2. To describe the production and sedimentation of the aerosol we use a time function which depends on latitude as well as the season and time after eruption, introduced in section 2.3.

As an assessment of the strength  $a^*$  of a volcano eruption, the Volcanic Explosivity Index ( $VEI$ ), provided by Simkin *et al.* (1981) and actualized by Siebert (1993), is used where  $a^* = 10^{VEI}$  for large eruptions with a column height of at least 10 to 25 km ( $VEI \geq 4$ ) and zero otherwise. We neglect eruptions with  $VEI \leq 3$  because they are not supposed to inject precursors of aerosols into the stratosphere (Simkin *et al.*, 1981). The actualized version also takes into account the results of Robock and Free (1995) who argue that the Mount St. Helens eruption (1982) was only of  $VEI = 4$  instead of 5 and Agung eruption (1963) was of  $VEI = 6$  instead of 4. These two examples show that it is very difficult to get reliable information about the strength of eruptions before the period of detailed instrumental observations. Nevertheless, for some strong volcanic eruptions the stratospheric mass loading is known from observations or is estimated indirectly. Since the middle of the nineteenth century six volcanic eruptions occurred with a  $VEI$  of 6. For all these eruptions estimates of stratospheric aerosol mass loading are provided by several researchers using different methods. Stothers (1996) presents an overview of the results and a comparison with his own investigations. We list these estimated stratospheric aerosol loading in Table 1. The averaged stratospheric aerosol loadings of the six most recent eruptions with  $VEI = 6$  amounts to  $\mu = 24.8 Tg$ . Assuming that a volcanic eruption with  $VEI = 6$  leads exactly to an aerosol loading of  $25 Tg$  we obtain the following equation to correct the  $VEI$  data in respect to the estimated stratospheric aerosol loading  $M$ :

$$VEI_{correct} = 4 + \log_{10}(4 Tg^{-1} \cdot M). \quad (3)$$

The corrected  $VEI$  values are listed in the last column of Table 1. For volcanoes with  $VEI < 6$  estimates of stratospheric mass loading exist, too (Stothers, 1996). We also correct the  $VEI$  of these volcanoes with respect to the observations using equation (3). The results for the strongest observed eruptions since 1880 are listed in Table 2. For our further investigations we use the series with corrected  $VEI$  values.

Table 1. Volcanic aerosol loading of the stratosphere in  $Tg$  after Stothers (1996) for volcanoes with  $VEI = 6$  and corrected  $VEI$  after equation 3.

Volcano	Year of eruption	Mass loading in $Tg$	Corrected $VEI$
Krakatau	1883	44	6.25
Santa Maria	1902	30	6.08
Katmai	1912	11	5.64
Agung	1963	20	5.9
El Chichón	1982	14	5.75
Pinatubo	1991	30	6.08
Average		24.8	5.95

Table 2. Volcanic aerosol loading of the stratosphere in  $Tg$  after Stothers (1996) for strong volcanic eruptions since 1880 with  $VEI < 6$  and corrected  $VEI$  after equation 3.

Volcano	Year of eruption	Mass loading in $Tg$	Corrected $VEI$
Unidentified <sup>a)</sup>	1890	6	5.38
Soufriere/Pele	1902	5	5.3
Ksudach	1907	4	5.2
Puyehue	1921	2	4.9
Komakatake	1929	4	5.2
Paluweh	1928	3	5.08
Quizapa	1932	3	5.08
Bezymianny	1956	not significant	4 <sup>b)</sup>
Fernandino	1968	6 <sup>c)</sup>	5.38
Fuego	1974	5 <sup>c)</sup>	5.3
Average		4.2 <sup>d)</sup>	5.2 <sup>d)</sup>

a) Stothers (1996) gives a range of 6 to 24  $Tg$  which depends on the latitude of eruption. Since we suppose that Bogoslof ( $54^\circ N$ ) may be the unidentified volcano, we use the smallest estimate of 6  $Tg$  according to the latitude of eruption.

b)  $VEI = 4$  corresponds to  $M = .25Tg$ .

c) Values are taken from a scaling of the observed  $AOD$  compared to the observations of Mt. Pinatubo (1991).

d) Bezymianny eruption not considered.

## 2.2. Stratospheric transport of volcanic aerosol

Transport processes in the stratosphere seem to be very complicated and are not known in detail. Therefore, usually observed  $AOD$  patterns are used to drive GCMs (Stenchikov *et al.*, 1997). Because the volcanic aerosol reaches mainly the lower stratosphere with a maximum concentration at an altitude about 21 km in the tropics and about 10 km in the polar regions (Hitchmann *et al.*, 1994), one may try to use stratospheric circulation models to simulate aerosol distributions. According to Plumb (1996), however, there is enough information available to create realistic formulations of the stratospheric transport without the necessity to solve the primitive equations. We perform this with a non-local diffusion formalism as it is introduced in boundary layer meteorology by Stull (1984). Considering  $m$  equal-area latitude belts, each containing an aerosol amount  $a_i(n)$  (given as mass concentration) at the time  $n$ , we can define a transient  $m \times m$  matrix  $\mathbf{A}_1$  to describe the temporal evolution of a spatial pattern by

$$\mathbf{a}(n+1) = \mathbf{A}_1 \mathbf{a}(n) \quad (4)$$

where the vector  $\mathbf{a}(n)$  is given as  $\mathbf{a}(n) = (a_1(n), a_2(n), \dots, a_m(n))$ . The initial conditions are the aerosol loading  $a_i^*(0) = a^*$  in the latitude belt of eruption  $i = i^*$  at the time of eruption  $n = 0$ .

The transient matrix does not need to be constant in time. Instead, the matrix rather depends on the annual cycle. Therefore we rewrite equation (4) to introduce a dependence on the season  $s$ :

$$\mathbf{a}(n+1) = \mathbf{A}_s \mathbf{a}(n). \quad (5)$$

Note that the time step  $n$  is independent from the season.

Now we consider 16 latitude belts and four seasons. So the transient matrix consists of  $16 \times 16 \times 4 = 1024$  coefficients. This seems to be a compromise between the desired spatial resolution and the deficiency of information about the transport processes. To decrease the very high degree of freedom we introduce the following assumptions:

- If we assume symmetric seasons, there are only two different ones: an extreme one (a winter- and a summer hemisphere) and a moderate one without hemispheric differences. This reduces the amount of coefficients in the transient matrix to  $16 \times 16 + 16 \times 8 = 384$ .
- If we consider very short time steps, we can apply a local (non-isotropic) exchange. This means that only the diagonal and the first subdiagonals of the matrix are filled with non-zero elements. Therefore we have to know only  $2 \times 16 + 4 \times 15 = 92$  elements. Taking also into account the conservation of mass (i.e. the transport is without sources and sinks) the sum over any column or row of the matrix has to be unity. This leads to 30 independent coefficients.
- According to Hitchmann *et al.* (1994) we can distinguish between tropics (bordered by a pronounced mean aerosol gradient at about  $20^\circ\text{N}$  and  $20^\circ\text{S}$ ), extratropics, and polar regions (poleward of about  $60^\circ\text{N}$  and  $60^\circ\text{S}$ ), see Figure 1. By using 16 equal-area latitude belts, there are 6 belts between  $\pm 22^\circ$  representing the tropics, 8 belts that represent the extratropics and 2 representing the polar region ( $61^\circ - 90^\circ$ ).

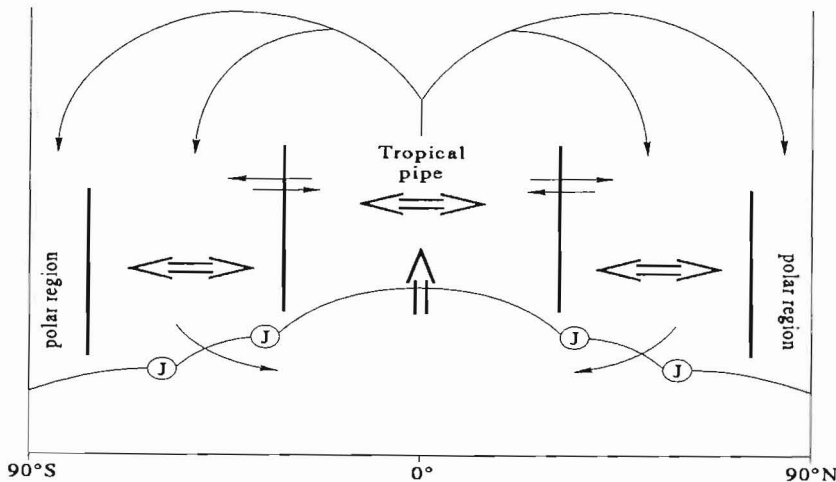


Fig. 1. Scheme of stratospheric mass transport processes (J=jetstream).

- Now we consider an isotropic transport within the tropics, anisotropic exchange between tropics and extratropics, isotropic transport within the extratropics (two seasons) and isotropic exchange between extratropics and polar regions in the summer- and winterhemisphere as well as during the moderate seasons. Together with the condition of conservation of mass this leads to only 8 independent coefficients (Table 3), which have to be taken from or estimated from literature.

Table 3. Exchange coefficients  $m_{i,k}$  for different regions in % per month.

tropics $\leftrightarrow$ tropics	91
tropics $\rightarrow$ extratropics	30
extratropics $\rightarrow$ tropics	7
extratropics $\leftrightarrow$ extratropics (winter-spring)	90
extratropics $\leftrightarrow$ extratropics (summer-fall)	45
extratropics $\leftrightarrow$ winter polar vortex	10
extratropics $\leftrightarrow$ summer polar region	45
extratropics $\leftrightarrow$ polar region in moderate season	23

We assume that the mixing within the tropical region leads to a nearly homogeneous distribution (less than 10% deviation from the mean value) within 3 months after an eruption that occurs between  $\pm 7^\circ$  latitude. This is realized by an exchange coefficient of 91% per month.

Volk *et al.* (1996) calculated an entrainment rate from extratropics into tropics of about 7% from observations. Because this value does not change between an altitude of about 16 to 21 km we assume that this is adequate for our purpose. The same authors found an average detrainment rate of 5% to 35% with a pronounced altitudinal dependence. An analysis by Waugh (1996) leads to a transport rate from the tropics to the Northern Hemisphere extratropics of about 8 to 10% of the tropical mass per month. Because the uncertainty of these estimations is about 50%, the results are in reasonable agreement. Assuming a homogeneous aerosol distribution within the six tropical latitude belts considered in our approximation, the exchange coefficients from the tropical border to the extratropics follow to be three times the transport rate per tropical mass. This leads to about 24% to 30% per month. Considering that the distribution of aerosol within the tropics is not exactly homogeneous we use the upper estimate as the exchange coefficient.

Boering *et al.* (1994) give an extratropical mixing time of about 2 to 3 months. According to this we use an extratropical exchange coefficient of 90% per month. Then a stratospheric aerosol amount entering the extratropics is distributed nearly homogeneously (with  $\pm 5\%$  deviation of the average value) within the extratropics after 80 days. Because circulation is more vigorous in winter and spring than in other seasons, Hitchmann *et al.* (1994) found that extratropical radiation extinction in winter-spring and summer-fall hemispheres differ by about 20 to 50%. To consider the lower exchange in summer and spring we assume the extratropical exchange coefficients in these seasons to be 45% per month which is half of the winter/spring value. The exchange coefficient between the extratropics and the summer polar region is supposed to be the same as the extratropical exchange coefficient in summer. In winter the polar vortex suppresses most of the exchange. Nevertheless, since the mean aerosol cloud in this latitude region is mainly in a height of about 8 to 16 km (Hitchmann *et al.*, 1994) where the polar vortex is not tight, we assume an exchange coefficient of about 10% per month in winter time. For spring and fall (April/May and October/November) we use an average exchange coefficient of 23% per month.

Given the exchange coefficients between latitude belt  $i$  and  $k$  in per cent per month  $m_{i,k}$ , it is easy to get the exchange coefficients  $a_{i,k}$  in per cent per time step as

$$(1 - a_{i,k})^\mu = 1 - m_{i,k} \quad (6)$$

if one month equals  $\mu$  time steps. For practical calculations we take 180 time steps per year to fill the transient matrix and use  $\mathbf{A}_s^3$  for calculations with 60 time steps per year. Note that  $\mathbf{A}_s^3$  is now a non-local transient matrix.

### 2.3. Residence time of volcanic aerosol

Explosive volcanism injects precursors of aerosols like sulfate dioxide ( $SO_2$ ) into the stratosphere which are converted into stratospheric aerosol by gas-to-particle conversion. This leads to very small particles which coagulate to larger ones. Eventually the large particles fall out by sedimentation (Kasten, 1968).

The interaction of all these microphysical processes is extremely complicated and hard to handle in detail. Furthermore, the radiative properties of the aerosol depend not only on the concentration but also on the size distribution and shape of the particles, which hampers the derivation of a complete microphysical model.

Fortunately we are not primarily interested in the microphysical processes, but in the impact of volcanism on the climate. Therefore we use macroscopic observational information to deal with that problem, i.e. we suggest a certain formulation of the temporal evolution of an aerosol cloud and calibrate it with respect to observed data.

In fact, we assume a linear increase of the total aerosol mass up to 5 months after eruption leading to a maximum mass according to the strength of the eruption. This seems to be a compromise between the estimates of build-up times to the peak AOD reaching from one month (Pinto *et al.*, 1989) over six months (Deshler *et al.*, 1993) to nine to twelve months (Ardanuy *et al.*, 1992). Grant *et al.* (1996) found a peak loading 20 weeks after the Pinatubo eruption in 1991.

After that we assume a mainly exponential decrease of the stratospheric AOD. According to Ardanuy *et al.* (1992) and Grant *et al.* (1996) we use a mean e-folding time of stratospheric aerosol of one year. This is supported by more detailed observations of the Pinatubo stratospheric aerosol cloud by Lambert *et al.* (1993). An optical depth of  $5.5 \cdot 10^{-3}$  in April 1992 and  $4.4 \cdot 10^{-3}$  in July 1992 was observed. According to these observations an e-folding time of 13.44 months can be estimated. Nevertheless, Hofmann and Rosen (1987) found shorter decay times for the Fuego aerosols (Guatemala, 1974) of about 8 to 10 months and about 10 to 12 months for the El Chichón eruption (1982).

The major sink of stratospheric aerosol is the stratosphere-troposphere flux of air which is described by Rosenlof and Holton (1993) and Holton *et al.* (1995) to be in the order of  $10^9$  to  $10^{10} \text{ kg/s}$  in the extratropics (Table 4). Within the tropics tropospheric air enters the stratosphere and thus hampers the sedimentation of aerosol. Therefore the tropical stratosphere is often seen as a tropical stratospheric reservoir (TSR, Grant *et al.*, 1996). According to Grant *et al.* (1996) we assume that sedimentation is not an important aerosol removing mechanism within the TSR. In fact, we allow no sedimentation in the tropical regions and therefore have to increase the removal rates in the extra-tropics to reproduce the observed average removal e-folding times. Thus we need an e-folding time of only 5 months in the extratropics to obtain the latitudinal averaged e-folding time of 12.2 months for the Pinatubo eruption in 1991.

Table 4. Vertical exchange of air between stratosphere and troposphere in  $\frac{10^8 \text{ kg}}{\text{s}}$  (taken from Rosenlof and Holton, 1993)

	DJF	JJA	Annual average
N hemisphere extra-tropics	-81	-26	-53.5
Tropics	114	56	85
S hemisphere extratropics	-33	-30	-31.5

By using this information we may describe the impact of all microphysical processes on the temporal evolution of a volcanic stratospheric cloud by one function that depends on the latitude belt  $i$ , the season  $s$ , and the time after eruption  $n$ .

An additional sink in the winter polar vortex is wash-out by polar stratospheric clouds (PSC's). This is neglected because of the short residence time and the small spatial fraction covered by PSC's (Volk, 1998). The calibration coefficient  $p_1$  in equation (2) can be taken from fitting the parameterization results to observations as described in section 4.

### 3. Radiative forcing

Radiative processes within the atmosphere are very complicated. Nevertheless, handsome analytic approximations like "delta-Eddington" (Joseph *et al.*, 1976) and two-stream approximations (Coakley and Chýlek, 1975) exist; for an overview see Meador and Weaver (1980). For homogeneous plane-parallel layers these approximations lead to linear differential equations with constant coefficients and, in consequence, to exponential solutions for vertical energy fluxes. The applicability of these solutions is usually limited to certain ranges of the optical properties like *AOD*, single scattering albedo and the moments of the scattering phase function. Thus, we are faced with two problems. First, we neither know the optical parameters of the aerosol cloud nor do we know their temporal change, apart from the *AOD*. Second, we cannot assume a plane-parallel layer but have to consider a spherical layer and have to deal with large zenith angles, i.e. close to  $90^\circ$ . Thus, we decide to assume an exponential behaviour as it is supposed in the most simple solutions of the radiation transfer equation and adapt it to observations. The weakening effect of a ray passing through a layer follows from the RTE as

$$N_b = N_t \exp \left\{ - \int_{z_b}^{z_t} \sigma_E \omega dz \right\} \quad (7)$$

with

- $N_b$  = radiative energy flux at the bottom of the aerosol layer,
- $N_t$  = radiative energy flux at the top of the aerosol layer,
- $z_t$  = top of the aerosol layer,
- $z_b$  = bottom of the aerosol layer,
- $\omega$  = ratio between the vertical thickness of the layer and the ray path, and
- $\sigma_E(z)$  = extinction coefficient within the aerosol layer.

Although this solution is more realistic than Lacis' *et al.* (1992) approximation which does neither depend on  $N_t$  nor on the factor  $\omega$ , we also neglect an explicit consideration of forward scattered radiation. Anyway, if the part of forward scattered radiation is proportional to the extinction we are not wrong if we use equation (7) with a calibration coefficient  $p_2$  to be estimated from observations (see section 4).

Regarding  $\sigma_E$  as the sum of the extinction coefficients with and without volcanic aerosol,  $\sigma_v$  and  $\sigma_0$  respectively, we can rewrite equation (7) as

$$N_v = N_0 \exp \left\{ - \int_{z_b}^{z_t} \sigma_v \omega dz \right\} \quad (8)$$

with  $N_0$  = radiative energy flux at the bottom of the undisturbed layer (without any volcanic aerosol) and  $N_v$  = radiative energy flux at the bottom of the volcanic aerosol layer. Because of the very weak dependence of  $\omega$  from  $z$  within the stratosphere we can further write

$$\int_{z_b}^{z_t} \sigma_v \omega dz = AOD \cdot \omega. \quad (9)$$

The energy flux change  $\Delta N$  with respect to volcanic stratospheric aerosol is now given as the difference between  $N_0$  and  $N_v$ . To obtain an approximated forcing  $\Delta Q$ , the vertical portion of the downward energy flux change

$$\Delta N_{\perp} = N_{0,\perp} \cdot [1 - \exp(-AOD \omega)] \quad (10)$$

is then multiplied by the planetary coalbedo  $1 - \alpha_p$ . The observed volcanic  $AOD$  has to be multiplied by the calibration coefficient  $p_2$  to consider that it is a bulk property and that we neglect an explicit description of the scattered radiation. Thus we get

$$\Delta Q = N_{0,\perp} (1 - \alpha_p) [1 - \exp(-AOD \cdot \omega \cdot p_2)]. \quad (11)$$

Now this equation has to be averaged over the time steps and latitude belts. If the time steps and latitude belts are chosen to be small,  $\Delta Q$  depends weakly on latitude and time within the latitude belts  $i$  and time steps  $n$ . Thus, we approximate all variables by their corresponding latitude-belt and time-step averages. Therefore  $AOD$  depends on  $i$  and  $n$ , while all other variables depend on  $i$  and have an annual cycle. The mean annual cycles of  $N_{0,\perp}$  and  $1 - \alpha_p$  are taken from a Fourier-Legendre-decomposition applied by North and Coakley (1979).

The ratio  $\omega$  between the ray path  $l$  and the thickness of the layer  $d$  depends on the zenith angle  $\Theta$  of the incoming solar radiation. It is usually set to  $\omega = 1/\cos(\Theta)$  which is applicable for  $\Theta < 80^\circ$ . For  $\Theta$  close to  $90^\circ$ , i.e. at sunrise and sunset,  $1/\cos(\Theta)$  diverges and therefore this parameterization would overestimate the forcing. To meet this problem, we consider the curvature of the stratospheric aerosol layer and use a more realistic parameterization of  $\omega$ .

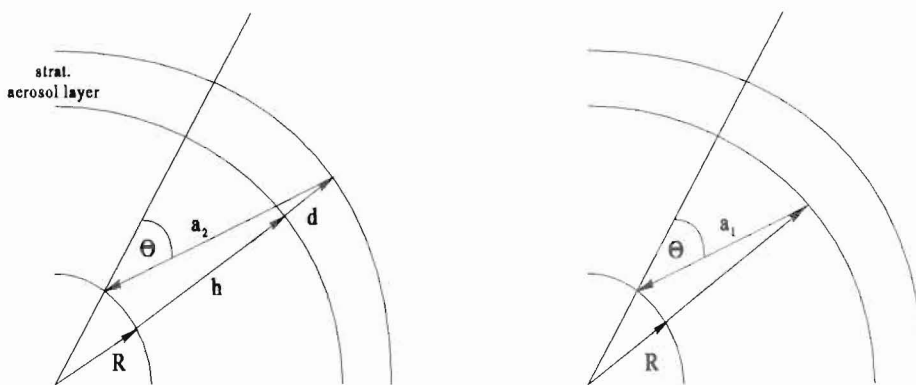


Fig. 2. Scheme of extended ray path in a spherical layer. A ray from zenith angle  $\Theta$  passes through a layer of thickness  $d$  with a bottom height  $h$  above ground. The ray path is given by  $a_2 - a_1$ .

We consider no refraction and therefore the ray path is a straight line. According to observations (Deshler, 1993) we regard the aerosol layer as homogeneous with a thickness  $d = 10\text{km}$  and a bottom height  $h$  of  $15\text{km}$  above the Earth surface. Therefore the layer has a curvature

with the radius  $R_b = R + h$  at the bottom and  $R_t = R_b + d$  at the top, if  $R$  is the Earth radius. According to Figure 2 the ray path  $l$  is given by

$$\begin{aligned} l &= a_2 - a_1 \\ a_1 &= \frac{R_b}{\sin(\pi - \Theta)} \sin \left\{ \Theta - \arcsin \left[ \frac{R}{R_b} \sin(\pi - \Theta) \right] \right\} \\ a_2 &= \frac{R_t}{\sin(\pi - \Theta)} \sin \left\{ \Theta - \arcsin \left[ \frac{R}{R_t} \sin(\pi - \Theta) \right] \right\}. \end{aligned} \quad (12)$$

$\Theta$  itself is a function of latitude  $\varphi$ , the time within the year  $t_y$ , and the time within the day  $t_d$  (e.g. Monin, 1986):

$$\Theta = \arccos(\sin \delta \sin \varphi + \cos \delta \cos \varphi \cos \phi). \quad (13)$$

It can be approximated by the formulation given by Paltridge and Platt (1976)

$$\begin{aligned} \delta &= .006918 - .399912 \cos \vartheta + .070257 \sin \vartheta \\ &\quad - .006758 \cos 2\vartheta + .000907 \sin 2\vartheta \\ &\quad - .002697 \cos 3\vartheta + .001480 \sin 3\vartheta \end{aligned} \quad (14)$$

with

$$\begin{aligned} \vartheta &= 2 \pi t_y \\ \phi &= 2 \pi (t_d - 12h). \end{aligned} \quad (15)$$

On the time scales of interest a consideration of the time dependence within the day is not necessary. Therefore, in the next step, the ratio  $\omega$  is averaged over the day light period. The borders of the integral are taken from (13) under the condition  $\Theta = \pi/2$  which means sunrise and sunset and depend from latitude and time within the year. Inserting equation (14) in (13) and the resulting one in (12) we find an expression of  $\omega(t_y, \varphi)$  as a function of latitude and time within the year. Using this approximation,  $\omega$  is restricted to be smaller than 13 in the case of  $\Theta \rightarrow \frac{\pi}{2}$  (sun position at the horizon).

Although we use a crude approximation compared to detailed solutions of the RTE, we realize two important facts: the seasonal and spatial patterns of the undisturbed radiation uptake  $N_{0,\perp} \cdot (1 - \alpha_p)$  given by North and Coakley (1979) and the seasonal and spatial patterns of the ratio  $\omega$ .

## 4. Calibration and results

### 4.1. Time series of volcanic induced stratospheric aerosol optical depth

There are two coefficients to fit the parameterization to observations. The first one ( $p_1$ ) is given in equation (2) to fit the aerosol transport parameterization to observations given by Sato *et al.* (1993), Sato (1995), and Stothers (1996). Because the AOD values by Stothers (1996) are valid for the visible spectral range and the AOD values provided by Sato *et al.* (1993) and Sato (1995) relate to a wavelength of  $.55 \mu m$ , the latter ones have to be converted with a scale factor of 1.6 for comparison (Stothers, 1996). Thus we have two time series of volcanic stratospheric

*AOD* at our disposal. Since the calibration coefficient  $p_1$  affects only the magnitude of the spatio-temporal pattern we decide to choose it in a way to obtain the same annual and global average value for the year 1983 as Sato (1995). Accordingly we will get a realistic description of the globally and annually averaged influence of the El Chichón eruption as it is observed. Figure 3 shows the *AOD* time series of Stothers (1996), Sato (1995) and of this paper for four equal area latitude belts. The global mean time series are shown in Figure 4.

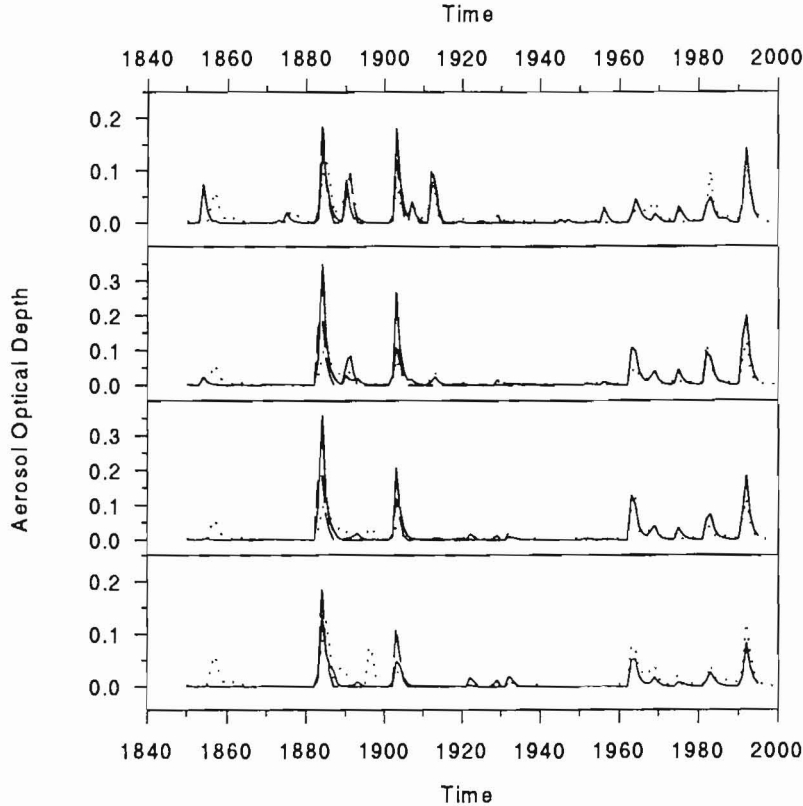


Fig. 3. Comparison of volcanic induced aerosol optical depth (*AOD*) time series for four equal area boxes. Top panel: northern hemisphere extra-tropics, second panel: northern hemisphere tropics, third panel: southern hemisphere tropics, bottom panel: southern hemisphere extra-tropics. Solid lines: this paper; dashed lines: Stothers (1996); dotted lines: Sato *et al.* (1993, 1995).

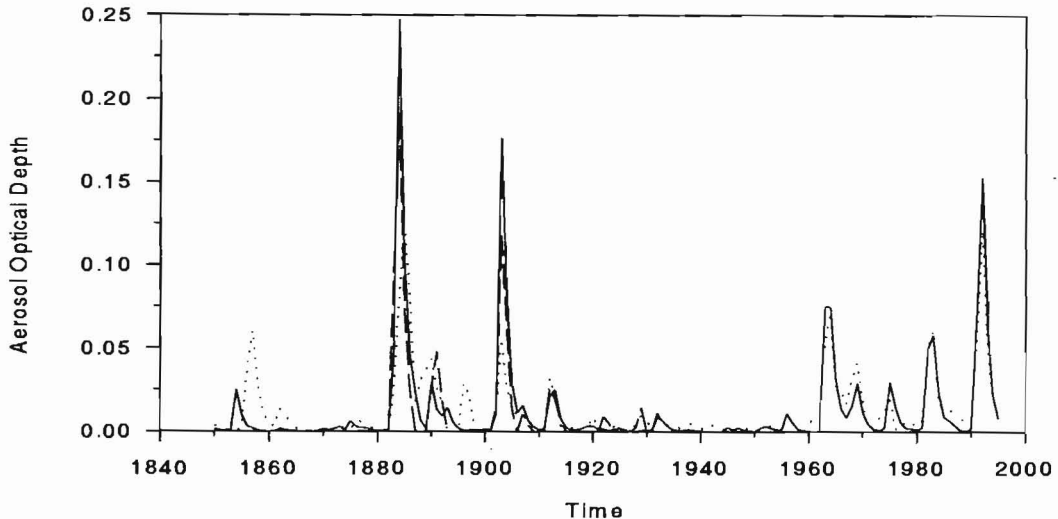


Fig. 4. Comparison of globally averaged volcanic *AOD* time series. Solid line: this paper; dashed line: Stothers (1996); dotted line: Sato (1995).

To obtain an objective measure of similarity of the different time series, we calculate linear correlation coefficients. These correlation coefficients are presented in Table 5. There are good linear correlations between the three time series on all regional scales considered. The *AOD* time series, calculated in this paper, is better correlated with the time series proposed by Stothers (1996) than with the time series published by Sato (1995). Apart from the Northern Hemisphere extra-tropics, correlations between the data of Sato (1995) and Stothers (1996) are not as high as data resulting from this paper compared with both of the other series, respectively. Nevertheless, all correlations are higher than those of the ice core volcanic index (*IVI*, Robock and Free, 1995) and the index of Sato (1995), which are quantified by Robock and Free (1995) to be .4 for the Northern Hemisphere and .54 for the Southern Hemisphere. Because the explained variance is the square of the correlation coefficient, these two series reach less than 50% of combined variance. In contrast to that, the approach of this paper reaches more than half of the combined variance with both the data from Sato (1995) and Stothers (1996), respectively.

Table 5. Linear correlations of the different volcanic *AOD* time series.

Time series	Time interval	Linear correlation coefficient				
		global	90° – 30°S	30° – 0°S	0° – 30°N	30° – 90°N
Sato / Stothers	1880 – 1933	.68	.57	.56	.64	.81
Sato / this paper	1850 – 1995	.77	.75	.71	.75	.76
Stothers / this paper	1880 – 1933	.94	.94	.90	.83	.90

#### 4.2. Time series of volcanic radiative forcing

To calibrate the radiative forcing parameterization, we compare the estimated forcing with observations and calculations from more sophisticated models. Dutton and Christy (1992) show that monthly clear-sky total solar irradiance at Mauna Loa, Hawaii, decreased about 5% after the Pinatubo eruption (June 1991) with a ten month average of 2.7%. The latter value corresponds to more than  $10 \text{ W/m}^2$  clear-sky forcing at the surface (at an elevation of about 3.400 m). Minnis *et al.* (1993) used ERBE data between  $\pm 40^\circ$  latitude and showed that in August 1991 the reflected shortwave radiation at the top of the atmosphere increased about  $10 \text{ W/m}^2$ .

Hansen *et al.* (1996) calculated a global and seasonal mean net radiation forcing of about  $4 \text{ W/m}^2$  from the end of 1991 to summer 1992 using a GCM. Graf *et al.* (1996) found the strongest volcanic forcing in summer polar regions with a magnitude of about  $5 \text{ W/m}^2$ , and no forcing at the winter polar regions performing equilibrium simulations with an atmosphere-ocean general circulation model (AOGCM). Realizing such differences even in sophisticated models, we choose the parameter  $p_2$  to obtain a magnitude of monthly and Northern Hemisphere tropical volcanic forcing of  $10 \text{ W/m}^2$  following the Pinatubo eruption (1991). This leads to a forcing of about  $5.1 \text{ W/m}^2$  in global average for the last quarter of 1991.

Using the time series of *AOD* provided by Sato (1995) and by Stothers (1996) and the crude radiation parameterization given by Lacis *et al.* (1992) (equation (1) in this paper), we get time series of volcanic forcing (in  $\text{W/m}^2$ ) for the same equal area latitude belts as they are used in Figure 3. These are presented in Figure 5. Figure 6 shows the related annual and global averages. The linear correlation coefficients of the different forcing time series are listed in Table 6. Because the parameterization by Lacis *et al.* (1992) is linear, the correlations between the forcings calculated from *AOD* series by Sato (1995) and by Stothers (1996) are the same as for the *AOD* series themselves and therefore not explicitly given in Table 6.

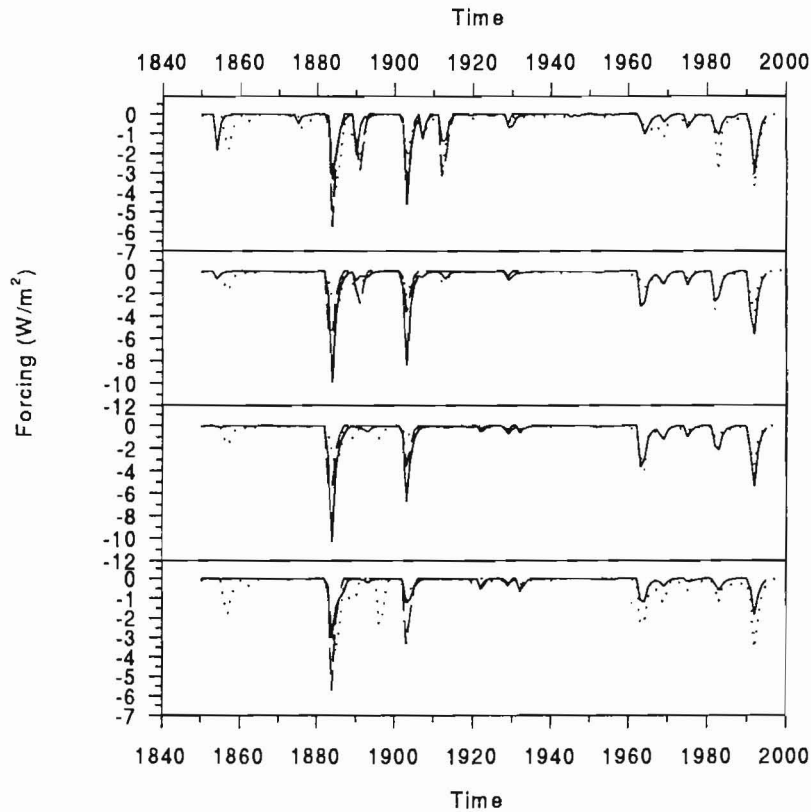


Fig. 5. Comparison of volcanic radiative forcing time series ( $W/m^2$ ) for four equal area latitude belts. Top panel: northern hemisphere extra-tropics, second panel: northern hemisphere tropics, third panel: southern hemisphere tropics, bottom panel: southern hemisphere extra-tropics. Solid lines: this paper; dashed lines: after Stothers (1996) and Lacis *et al.* (1992); dotted lines: after Sato (1995) and Lacis *et al.* (1992).

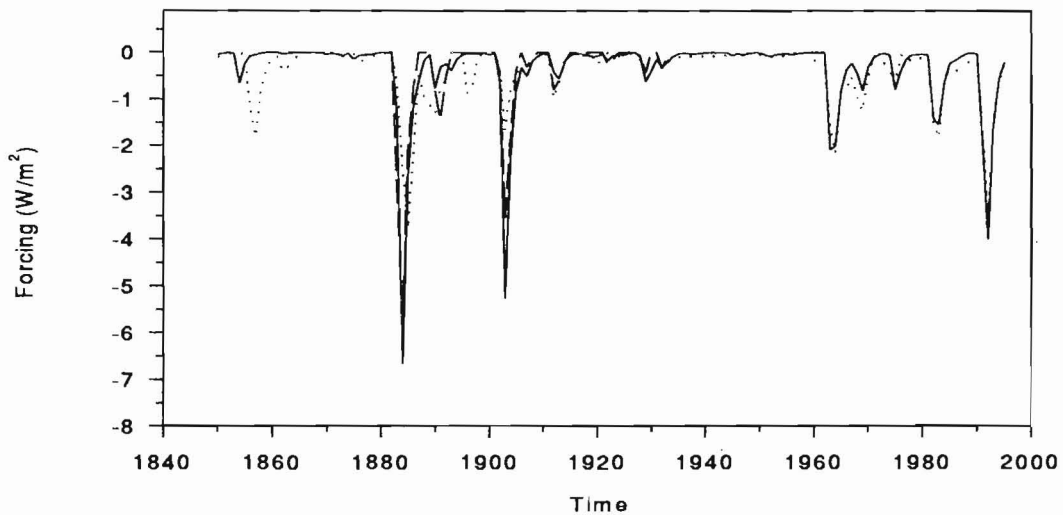


Fig. 6. Comparison of globally averaged volcanic radiative forcing time series ( $W/m^2$ ). Solid line: this paper; dashed line: after Stothers (1996) and Lacis *et al.* (1992); dotted lines: after Sato (1995) and Lacis *et al.* (1992).

Table 6. Linear correlation between the different volcanic forcing time series.

Time series	time interval	linear correlation coefficient				
		global	90° – 30°S	30° – 0°S	0° – 30°N	30° – 90°N
Sato / this paper	1850 – 1995	.75	.74	.70	.75	.72
Stothers / this paper	1880 – 1933	.94	.95	.90	.82	.86

Similar to the *AOD* series, the volcanic forcing series of Stothers (1996) and the approach of this paper are in better agreement, too, than the series of Stothers (1996) and Sato (1995) and our approach compared to the series of Sato (1995). Changes due to the non-linear radiation parameterization are very weak on the spatial and temporal scales under consideration. This will change considerably if one is interested in a more detailed spatial and temporal resolution, as will be seen in section 4.4.

#### 4.3. Long time series of volcanic radiative forcing

To study the volcanic influence on climate on a historical time scale, it is necessary to provide long time series of volcanic forcing. This problem is matched with the question of missing observations. Therefore Simkin *et al.* (1981) define a reporting index which is the number of volcanoes active per decade as a percentage of the number of volcanoes known at the start of each decade. Their reporting index, covering the last 600 years, shows 3 quasi-constant levels with two jumps in between. The first level is before 1500. Then knowledge of volcanoes increased dramatically so that a second level is reached lasting until the mid of the 18th century where the second jump leads to the third level. Thus, to avoid the influence of incomplete observation, we study forcing time series only since 1500. In principle, it would be no problem to estimate volcanic *AOD* and forcing time series from the beginning of the *VEI* series (about 10.000 years ago) where only coarse information about few eruptions is available: For the first 5 centuries A. D. only 6 eruptions with  $VEI=6$  are reported by Simkin *et al.* (1981). During the second and third 5 centuries A. D. only 2 eruptions with  $VEI \geq 6$  are reported. Furthermore it is important to know not only the year of eruption but also the month to make reasonable use of the aerosol-transport and radiation-transfer parameterization. Even for strong eruptions occurring before the last century this information is often not available. In order to investigate the lack of information about the month of eruption we compare the volcanic forcing of the Billy Mitchell eruption (Bougainville, 6.1° S, 155° E) in 1580 for the case that the eruption with  $VEI = 6$  occurred in January with the case that the eruption occurred in July. The results are given in Figure 7. It can clearly be seen, that the knowledge of the date of eruption (at least the month) is important to quantify the spatio-temporal patterns of the forcing. Therefore, evaluating long time series of volcanic forcing in the desired spatio-temporal resolution, needs further knowledge of the date of eruption. Although the spatio-temporal patterns of the forcing depend strongly on the month of eruption, a three-year average forcing (year of eruption and following 2 years) depends not significantly on the eruption date as can be seen in Table 7. The *t*-value for a significant difference on the 80% level is 1.294 which is not exceeded by any of the different average values given in Table 7. Thus, if we are only interested in volcanic forcing time series of a three year average and 4 latitude belts, we can estimate the forcing even if we know only the year of eruption but not the month. Annually averaged values of estimated volcanic forcing since 1500 are given in Figure 8.

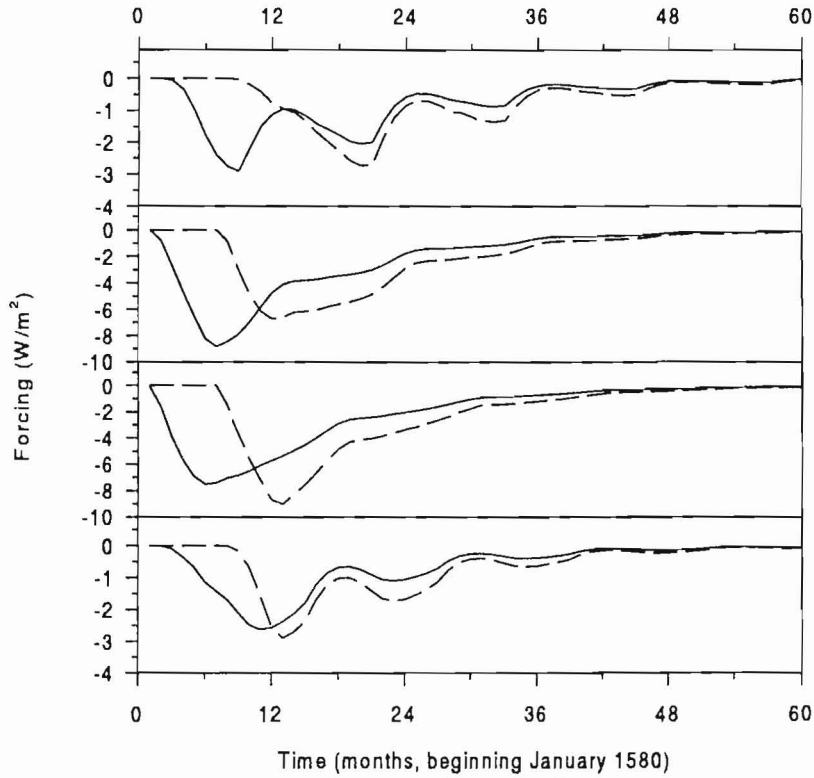


Fig. 7. Comparison of volcanic radiative forcing time series ( $W/m^2$ ) for four equal area boxes. Top panel: northern hemisphere extra-tropics, second panel: northern hemisphere tropics, third panel: southern hemisphere tropics, bottom panel: southern hemisphere extra-tropics. Solid lines: eruption occurred in January; Dashed lines: eruption occurred in July.

Table 7. Comparison of three year average forcing ( $W/m^2$ ) of a volcanic eruption occurring in January and July respectively.

Latitude belt	Januar eruption	July eruption	$\hat{t}$ -value of difference
$30^\circ - 30^\circ N$	-1.11	-.94	.89
$0^\circ - 30^\circ N$	-3.29	-2.98	.54
$0^\circ - 30^\circ S$	-3.28	-3.19	.15
$30^\circ - 90^\circ S$	-.98	-.96	.12

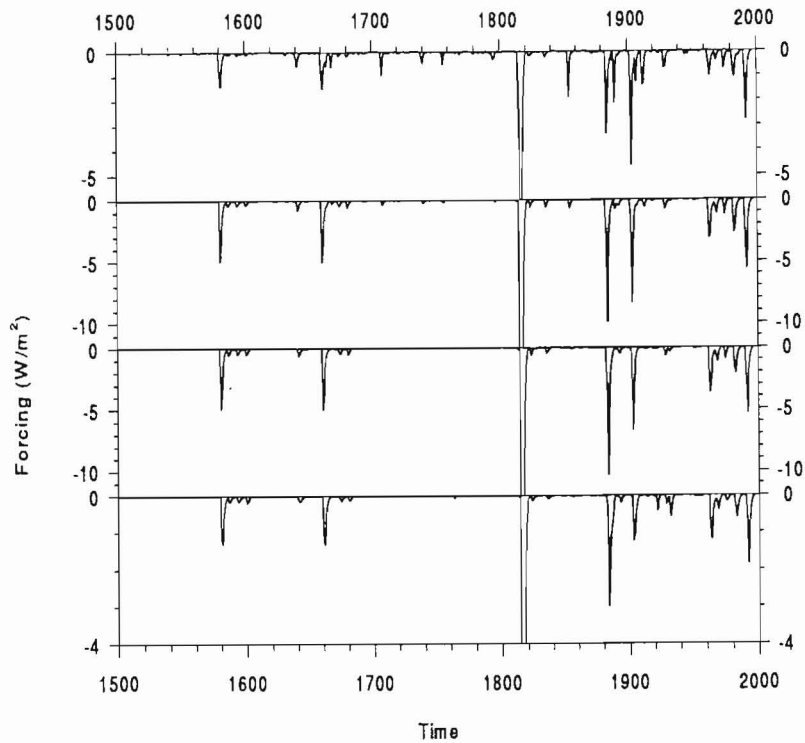


Fig. 8. Estimated volcanic radiative forcing time series ( $W/m^2$ ) for four equal area boxes since 1500. Top panel: northern hemisphere extra-tropics, second panel: northern hemisphere tropics, third panel: southern hemisphere tropics, bottom panel: southern hemisphere extra-tropics.

#### 4.4. Case studies

To give an idea of the spatio-temporal resolution of the parameterized *AOD* and forcing presented in this paper, we compare the results of two special episodes with the related results of Sato (1995) or Stothers (1996), in more detail. The first episode from January 1982 till June 1986 includes the El Chichón eruption ( $17.4^\circ$  N) in April 1982 which occurred nearly at the same latitude as the Pinatubo eruption ( $15.1^\circ$  N) in 1991. In contrast to the Pinatubo eruption the aerosol spreading of the El Chichón eruption was very assymmetrical, as can be seen from the data adapted from Sato (1995) in Figure 9a. Figure 9b shows the spatio-temporal *AOD* distribution as it follows from the parameterization of this paper. As can be seen both approximations are similar. Using the linear forcing parameterization by Lacis *et al.* (1992), the forcing pattern is a rescaled *AOD* pattern. Using the radiation-transfer parameterization of this paper, the forcing pattern shows an annual cycle (Figure 10), which is not as pronounced as in the case of the Billy Mitchell eruption (Figure 7 for comparison).

The second episode from January 1912 till June 1916 addresses the eruption of Katmai ( $58.3^\circ$  N) in June 1912. It has the same *VEI* as the El Chichón eruption in 1982 but due to its high latitude the aerosol spreading is completely different. We compare the *AOD* as it is provided by Sato *et al.* (1995) on a 24-point grid and by Stothers (1996) on a 3-box grid with our approach on a 16 equal area box resolution (Figure 11). Although Sato (1995) used 24 grid points, they distinguish only 3 latitude zones: Southern Hemisphere, Northern Hemisphere tropics and northern hemisphere extra-tropics. They find much larger signals in the Northern Hemisphere tropics than Stothers did and we do. In respect to north of  $45^\circ$  N the *AOD* series provided by Stothers is more similar to our results than the series from Sato (1995). In total, however, it can

be concluded that these differences are in the range of uncertainty typical for reconstructions of volcanic stratospheric *AOD*, although Sato (1995) as well as Stothers (1996) used observations, whereas we use a parameterization without any *AOD* observations of this period.

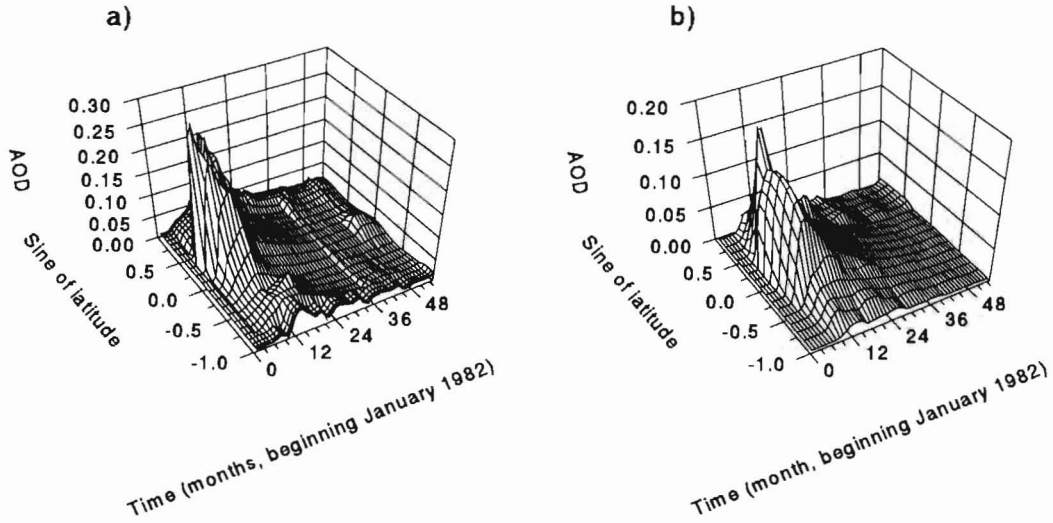


Fig. 9. Comparison of spatio-temporal *AOD* patterns from January 1982 until June 1986 (a) from Sato (1995), and (b) this paper.

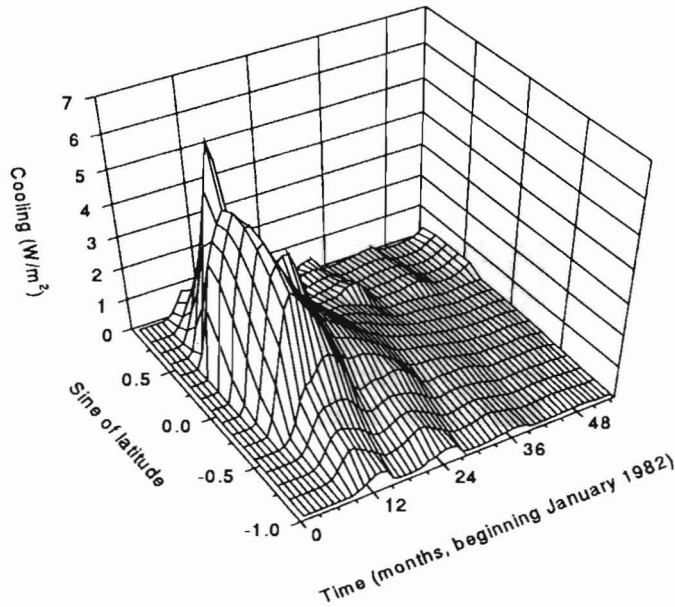


Fig. 10. Spatio-temporal pattern of volcanic forcing ( $W/m^2$ ) from January 1982 until June 1986.

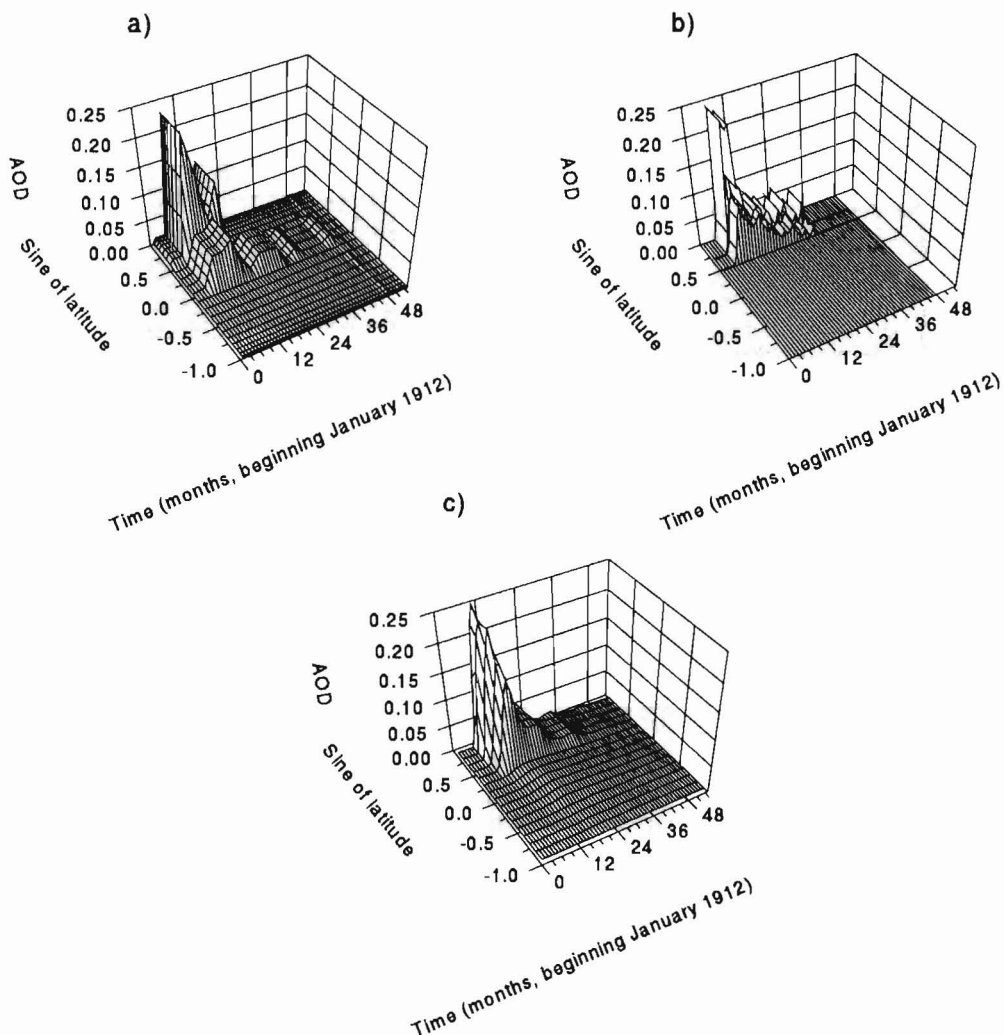


Fig. 11. Comparison of spatio-temporal *AOD* patterns from January 1912 until June 1916 (a) from Sato (1995), (b) from Stothers (1996), and (c) this paper.

These results encourage us to estimate forcing anomalies of historical eruptions like the Vesuvius eruption (Italy,  $VEI = 6$ ) in August 79 A. D. As can be seen in Figure 12a, *AOD* increases nearly homogeneously within the Northern Hemisphere extra-tropics. This is due to the little exchange from extratropics into tropics and into the winter polar vortex. In the following spring, sedimentation and transport to the polar region became effective and *AOD* declines dramatically. Figure 12b shows the spatio-temporal pattern of the related climate forcing which differs considerably from the *AOD* pattern. Despite of the decrease of the *AOD* in spring of the year 80, the forcing remains on a high level during the whole summer.

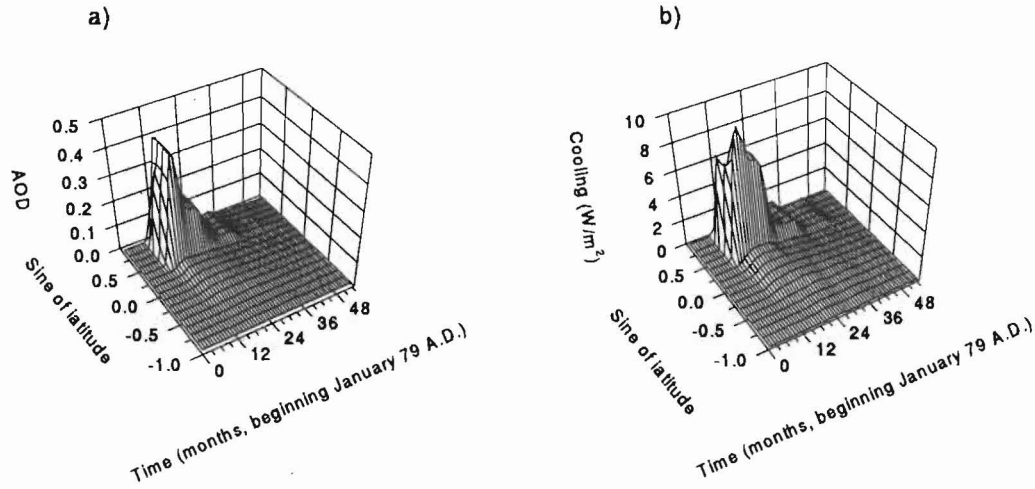


Fig. 12. Estimates of spatio-temporal patterns of (a) *AOD*, and (b) radiative forcing ( $W/m^2$ ) from January 79 A.D. until June 83 A.D.

## 5. Conclusion

Because strong explosive volcanic eruptions are known to have a pronounced impact on the climate it is important to estimate the spatio-temporal patterns of volcanic forcing. For the most recent eruptions instrumental observations from satellites and ground based measurements are available. For historical volcanic eruptions climate forcing has to be reconstructed. Therefore we introduced a stratospheric aerosol-transport parameterization based on nonlocal unisotropic diffusion. Exchange coefficients are obtained from recent studies of stratospheric mass transport. Strength, date and latitude of an eruption have to be known to apply the parameterization. We take this information from the *VEI* series, although the estimated strength of eruptions is not accurate, especially for eruptions a long time ago. Therefore, we correct the *VEI* with respect to observations for the strongest eruptions of the last century. While the parameterization is linear with respect to the strength of the eruption, errors in the estimated strength have no impact on the spatio-temporal structure of *AOD*. However, latitude and season of an eruption strongly affects the aerosol distribution and therefore the impact on the climate. If the required information is available we are able to reconstruct spatio-temporal patterns of *AOD* for volcanic eruptions not included in the calibration of the parameterization and even for historic eruptions. For most of the historic eruptions only the year of the eruption is known. This has an impact on the temporal structure of the forcing (Fig. 7). Nevertheless, as we have shown in an example (Table 7), the three year average forcing is not necessarily affected significantly by this lack of information.

The knowledge of volcanic stratospheric optical depth is necessary to estimate its climate impact, but the most important information is the forcing itself. It depends dramatically on the length of a ray path through the layer and the undisturbed radiation uptake. Also a pronounced aerosol cloud has no dramatic influence if it exists only in a winter polar region where there is nearly no radiation supply. Thus we introduce a radiation-transfer parameterization which takes into account these properties in their latitudinal and seasonal dependence to provide estimates of volcanic aerosol forcing.

We hope that our investigations of the volcanic climate forcing will be helpful for other researchers to study the relationship between volcanic forcing and the observed climate response.

## Acknowledgements

The authors wish to thank Michael C. Volk for his suggestions concerning stratospheric transport phenomena. The work is an extended part of a doctorate thesis of Jürgen Grieser, performed at the Centre for Environmental Research of Frankfurt University, Germany. The research was supported by the German Ministry for Education, Science, Research and Technology (Project number 07KFT120/9).

Readers interested in further details may visit our website at <http://www.rz.uni-frankfurt.de/~grieser>

## REFERENCES

- Ardanuy, P. E., H. Lee Kyle, and D. Hoyt, 1992. Global Relationships among the Earth's Radiation Budget, Cloudiness, Volcanic Aerosols, and Surface Temperature. *J. Clim.*, **5**, 1120-1139.
- Bradley, R. S., 1988. The Explosive Volcanic Eruption Signal in Northern Hemisphere Continental Temperature Records. *Clim. Change*, **12**, 221-243.
- Boering, K. A., B. C. Daube, Jr., S. C. Wofsy, M. Loewenstein, J. R. Podolske, and E. R. Keim, 1994. Tracer-tracer relationships and lower stratospheric dynamics: CO<sub>2</sub> and N<sub>2</sub>O correlations during SPADE. *Geophys. Res. Letters*, **21**, 2567-2570.
- Coakley Jr., J. A., and P. Chýlek, 1975. The two-stream approximation in radiative transfer: Including the angle of the incident radiation. *J. Atmos. Sci.*, **32**, 409-418.
- Cress, A., and C.-D. Schönwiese, 1992. Statistical signal and signal-to-noise assessments of the seasonal and regional patterns of global volcanism-temperature relationships. *Atmósfera*, **5**, 31-46.
- Deshler, T., B. J. Johnson, and W. R. Rozier, 1993. Balloonborne Measurements of Pinatubo Aerosol during 1991 and 1992 at 41° N: Vertical Profiles, Size Distribution, and Volatility. *Geophys. Res. Letters*, **20**, 1435-1438.
- Dutton, E. G. and J. R. Christy, 1992. Solar radiative forcing at selected locations and evidence for global lower tropospheric cooling following the eruptions of El Chichón and Pinatubo. *Geophys. Res. Letters*, **19**, 2313-2316.
- Dyer, A. J., and B. B. Hicks, 1968. Global spread of volcanic dust from the Bali eruption of 1963. *Quart. J. Royal Meteor. Soc.*, **94**, 545-554.
- Graf, H.-F., I. Kirchner, and I. Schult, 1996. Modelling Mt. Pinatubo Climate Effects. In NATO ASI Series, Vol. I 42, The Mount Pinatubo Eruption, Effects on the Atmosphere and Climate, Edited by Giorgio Fiocco, Daniele Fua, and Guido Visconti. Springer-Verlag Berlin, Heidelberg.
- Grant, W. B., E. V. Browell, C. S. Long, L. L. Stowe, R. G. Grainger, and A. Lambert, 1996. Use of volcanic aerosols to study the tropical stratospheric reservoir. *J. Geophys. Res.*, **101**, 3973-3988.
- Hansen, J. E., and A. A. Lacis, 1990. Sun and dust versus greenhouse gases: an assessment of their relative roles in global climate change. *Nature*, **346**, 713-719.
- Hansen, J. E., M. Sato, R. Ruedy, A. Lacis, K. Asamoah, S. Borenstein, E. Brown, B. Cairns, G. Caliri, M. Campbell, B. Curran, S. de Castro, L. Druryan, M. Fox, C. Jahnsson, J. Lerner, M. P. McCormick, R. Miller, P. Minnis, A. Morrison, L. Pandolfo, I. Ramberran, F. Zaucker, M. Robinson, P. Russel, K. Shah, P. Stone, I. Tegen, L. Thomason, J. Wilder, and H. Wilson,

1996. A Pinatubo Climate Modeling Investigation. In NATO ASI Series, Vol. I 42, The Mount Pinatubo Eruption, Effects on the Atmosphere and Climate, Edited by Giorgio Fiocco, Daniele Fua, and Guido Visconti. Springer-Verlag Berlin, Heidelberg.
- Hitchman, M. H., M. McKay, and C. R. Trepte, 1994. A climatology of stratospheric aerosol. *J. Geoph. Res.*, **99**, 20689-20700.
- Hofmann, D. J., and J. M. Rosen, 1987. On the prolonged lifetime of El Chichón sulfuric aerosol cloud. *J. Geoph. Res.*, **92**, 9825-9830.
- Holton, J. R., P. H. Haynes, M. E. McIntyre, A. R. Douglass, R. B. Rood, and L. Pfister, 1995. Stratosphere-Troposphere Exchange. *Rev. of Geoph.*, **33**, 403-439.
- Jones, P. D. and P. M. Kelly, 1996. The Effect of Tropical Explosive Volcanic Eruptions on Surface Air Temperature. In NATO ASI Series, Vol. I 42, The Mount Pinatubo Eruption, Effects on the Atmosphere and Climate, Edited by Giorgio Fiocco, Daniele Fua, and Guido Visconti. Springer-Verlag Berlin, Heidelberg.
- Joseph, J. H., W. J. Wiscombe, and J. A. Weinman, 1976. The Delta-Eddington Approximation for Radiative Flux Transfer. *J. Atmos. Sci.*, **33**, 2452-2459.
- Kasten, F., 1968. Falling Speed of Aerosol Particles. *J. Appl. Meteor.*, **7**, 944-947.
- Lacis, A. A., J. E. Hansen, and M. Sato, 1992. Climate forcing by stratospheric aerosols. *Geophys. Res. Letters*, **19**, 1607-1610.
- Lamb, H. H., 1970. Volcanic dust in the atmosphere, with a chronology of assessments of its meteorological significance. *Philos. Trans. R. Soc. London, A* **266**, 425-533.
- Lamb, H. H., 1977. Supplementary volcanic dust veil index assessments. *Clim. Monitor*, **6**, 57-67.
- Lamb, H. H., 1983. Update of the chronology of assessments of the volcanic dust veil index. *Clim. Monitor*, **12**, 79-90.
- Lambert, A., R. G. Grainger, J. J. Remedios, C. D. Rodgers, M. Corney, and F. W. Taylor, 1993. Measurements of the Evolution of the Mt. Pinatubo Aerosol Cloud by ISAMS. *Geophys. Res. Letters*, **20**, 1287-1290.
- McCormick, M. P., 1994. SAM II Aerosol data. NASA Langley Research Center. Mail Stop 157B. Hampton, Virginia 23681-0001. USA.
- McCormick, M. P., and P. H. Wang, 1987. Satellite measurements of stratospheric aerosols, in Transport Processes in the Middle Atmosphere, edited by G. Visconti and R. Garcia, pp. 103-120, D. Reidel, Norwell, Mass.
- McCormick, M. P., P. Hamill, T. J. Pepin, W. P. Chu, T. J. Swissler, and L. R. McMaster, 1979. Satellite studies of the stratospheric aerosol. *Bull. Am. Meteorol. Soc.*, **60**, 1038-1046.
- Meador, W. E., and W. R. Weaver, 1980. Two-stream approximations to radiative transfer in planetary atmospheres: A unified description of existing methods and a new improvement. *J. Atmos. Sci.*, **37**, 630-643.
- Minnis, P., E. F. Harrison, L. L. Stowe, G. G. Gibson, F. M. Denn, D. R. Doelling, and W. L. Smith, 1993. Radiative climate forcing by Mount Pinatubo eruption. *Science*, **259**, 1411-1415.
- Mitchell, J. M., Jr., 1970. A preliminary evaluation of atmospheric pollution as a cause of the global temperature fluctuation of the past century, in Global Effects of Environmental Pollution, edited by S. F. Singer, pp. 139-155, D. Reidel, Norwell, Mass.
- Monin, A. S., 1986. An Introduction to the Theory of Climate. D. Reidel Publishing Company, Dordrecht.

- Newhall, C. G., and S. Self, 1982. The volcanic explosivity index (*VEI*): An estimate of explosive magnitude for historical volcanism. *J. Geoph. Res.*, **87**, 1231-1238.
- North, G. R., and J. A. Coakley, Jr., 1979. Differences between Seasonal and Mean Annual Energy Balance Model Calculations of Climate and Climate Sensitivity. *J. Atmos. Sci.*, **36**, 1189-1204.
- Paltridge, G. W., and C. M. R. Platt, 1976. Radiative processes in meteorology and climatology. Elsevier Scientific Publishing Company, Amsterdam, Oxford, New York.
- Pinto, J. P., R. P. Turco, and O. B. Toon, 1989. Self-limiting physical and chemical effects in volcanic eruption clouds. *J. Geoph. Res.*, **94**, 11165-11174.
- Plumb, R. A., 1996. A "tropical pipe" model of stratospheric transport. *J. Geoph. Res.*, **101**, 3957-3972.
- Rind, D., 1996. The Potential for Modeling the Effects of Different Forcing Factors on Climate During the Past 2000 Years. In NATO ASI Series. Vol I 41, Climate Variations and Forcing Mechanisms of the last 2000 Years. Edited by Philip D. Jones, Raymond S. Bradley, and Jean Jouzel. Springer-Verlag Berlin Heidelberg, 1996.
- Robock, A. and M. P. Free, 1995. Ice cores as an index of global volcanism from 1850 to the present, *J. Geoph. Res.*, **100**, 11549-11567.
- Rosenlof, K. H., and J. R. Holton, 1993. Estimates of the stratospheric residual circulation using the downward control principle. *J. Geoph. Res.*, **98**, 465-479.
- Sato, M., J. E. Hansen, M. P. McCormic, and J. B. Pollack, 1993. Stratospheric Aerosol Optical Depths. 1850-1990. *J. Geoph. Res.*, **98**, 22987-22994.
- Sato, M., 1995. Update of Stratospheric Aerosol Optical Depths. On: <http://www.giss.nasa.gov/data/strataer/STRATAER.table.txt>.
- Schönwiese, C.-D., 1988. Volcanic activity parameters and volcanism-climate relationships within recent centuries. *Atmósfera*, **1**, 141-156.
- Siebert, L., 1993. Private Communication.
- Simkin, T., L. Siebert, L. McClelland, D. Bridge, C. Newhall, and J. H. Latter, 1981. Volcanoes of the World. Hutchinson Ross Publishing Company. Stroudsburg. Pennsylvania.
- Stenchikov, G. L., I. Kirchner, A. Robock, H.-F. Graf, J. C. Antuna, R. Grainger, A. Lambert, and L. Thomason, 1997. Radiative Forcing from the 1991 Mount Pinatubo Volcanic Eruption. MPI Report No. 231. Max Planck Institute for Meteorology, Hamburg, Germany.
- Stommel, H. and E. Stommel, 1979. The year without summer. *Sci. Amer.*, **240**, 176-186.
- Stothers, R. B., 1996. Major optical depth perturbations to the stratosphere from volcanic eruptions: Pyrheliometric period. 1881-1960, *J. Geoph. Res.*, **101**, 3901-3920.
- Stull, R., 1984. Transient turbulence theory. Part 1: the concept of eddy mixing across finite distances. *J. Atmos. Sci.*, **41**, 3351-3367.
- Tol, R. S. J. and A. F. De Vos, 1998. A Bayesian Statistical Analysis of the Enhanced Greenhouse Effect. *Clim. Change*, **38**, 87-112.
- Volk, M. C., J. W. Elkins, D. W. Fahey, R. J. Salawith, G. S. Dutton, J. M. Gilligan, M. H. Proffit, M. Loewenstein, J. R. Podolske, K. Minschwaner, J. J. Margitan, and K. R. Chan, 1996. Quantifying transport between the tropical and mid-latitude lower stratosphere. *Science*, **272**, 1763-1768.
- Volk, M. C., 1998. Private Communication.
- Waugh, D. W., 1996. Seasonal variation of isentropic transport out of the tropical stratosphere. *J. Geophys. Res.*, **101**, 4007-4023.